

Interner Bericht
DESY F41-69/2
Juni 1969

DESY-Bibliothek
30. JUNI 1969 ✓

Investigation of Optical Properties of Alkali Halides
and Solid Rare Gases by Synchrotron Radiation

R. Haensel

Physikalisches Staatsinstitut

II. Institut für Experimentalphysik, Hamburg

A lecture to be given at the Conference "Optical Properties of Solids"
June 29 - July 12, 1969 in Chania, Crete, Greece

INVESTIGATION OF OPTICAL PROPERTIES OF ALKALI HALIDES
AND SOLID RARE GASES BY SYNCHROTRON RADIATION

R. Haensel

Physikalisches Staatsinstitut, II. Institut
für Experimentalphysik der Universität Hamburg

ABSTRACT

Optical absorption spectra of inner shell transitions in alkali halides and solid rare gases have been obtained by the use of synchrotron radiation in the photon energy range 10 to 260 eV. For the alkali halides the results are compared with those in the fundamental absorption region, for the solid rare gases with the corresponding atomic transitions. The discussion of the results includes band structure calculations as well as exciton theory. In the experimental part some remarks are made on the characteristics of synchrotron radiation.

I. INTRODUCTION

Alkali halides and rare gas solids are formed from ions or atoms respectively which have completely filled atomic shells, and whose electrons, therefore, are closely bound to the nucleus. As a result there is a big energy gap between the occupied valence band states and the unoccupied conduction band states. Because of the big band gap these solids are transparent in the visible and have the onset of optical absorption in the vacuum ultraviolet. There are two reasons for the rapid growth of interest in the optical behaviour of these wide band gap materials during the last few years. One reason is the development of experimental techniques which has allowed more and more refined experiments. The second reason is the development of band structure calculations, which are now available for nearly all alkali halides and solid rare gases. Both developments are closely connected, for on the one hand the band calculations stimulated the experimentalists to compare experimental results with theoretical predictions. On the other hand the theoreticians used experimental values (e.g. of band gap energy) to adjust certain parameters in their calculations. Because of the big binding energy of the valence electrons the wavefunctions are highly localized (in the alkali halides at the halogen ion) and can be theoretically treated like the core states by a tight binding approximation. The valence bands are relatively flat and their width is much smaller than the band gap energy. The conduction band states are composed of the

unoccupied atomic states; because of the overlapping of the wavefunctions of neighbouring atoms they are spread over both the negative and positive ions. As the band calculations give results on the energy eigenstates of an electron in the conduction band with a filled valence band, they describe only interband transitions correctly. In large band gap materials with a low dielectric constant however, transitions play a big role where the hole, left by the excited electron, is not completely screened by the surrounding valence electrons but forms bound states together with the excited electron. These states are called excitons.

Excitons may be described with the help of two different models¹: The Frenkel picture describes the excitons as being built up of atomic wavefunctions. The Wannier-Mott picture describes it as a hole surrounded by the electron at a distance of the order of the lattice constant. The Wannier-Mott excitons form hydrogen-like eigenstate series, which converge towards certain singularities in the continuum conduction band. In our case an intermediate picture between these two boundary models has to be applied: Baldini² found that in valence band transitions of the solid rare gases, the first exciton is very close to the first atomic transition in the gas, but he also saw exciton series which are especially clear in solid xenon. In alkali halides exciton series have also been seen e.g. by Fischer and Hilsch.³ Band calculations covering the conduction band states are available for LiF^{4,5}, LiCl⁶, LiBr⁷, LiJ⁸, NaCl^{6,9,10}, NaBr⁷, NaJ⁸, KCl^{6,11-13}, KBr⁷, KJ¹⁴, RbCl⁷, RbBr⁷, CsJ^{15,16}, and for Ar¹⁷⁻¹⁹, Kr²⁰, and Xe²¹.

A review of the theoretical and experimental problems involved in the investigation of optical properties of alkali halides and solid rare gases may be found in papers by Knox and Teegarden²² and Baldini.²

II. VALENCE BAND AND CORE SHELL TRANSITIONS

The bulk of experimental material of optical properties of alkali halides and solid rare gases is available on transitions from the valence band. The valence band is built up of p-symmetric states. As the lowest part of the conduction band is mainly s-symmetric, the onset of optical absorption mainly shows structure due to transitions between these states including the excitons. As different transitions may have initial states at different points of the valence band, the optical absorption structure in the fundamental absorption region does not directly give a picture of the conduction band structure but of the combined valence- and conduction-band structure. Since the valence states have p-like symmetry wavefunctions concentrated at the halogen ion, the result is that only transitions into s- and d-symmetric final states, whose wavefunctions have a considerable weight at the halogen ion, can be observed. To get information on the other states in the conduction band, transitions from the core levels on both ions with different symmetry have to be studied additionally. Transitions from p-symmetric core states are also interesting. As the core bands

are completely flat a comparison of the absorption from the p-symmetric valence and the p-symmetric core states should help in the identification of the point of the Brillouin zone scheme at which the transition occurs.

The threshold energies for core excitation from the different subshells in the alkali halides and rare gases in the energy range up to 500 eV are compiled in Fig. 1. Most of the energy values give the onset of absorption based on optical measurements, the rest are values of the binding energy taken from the tables of Bearden and Burr.²³ The observable fine structure in absorption spectra investigated by transitions from very deep lying levels (threshold energy > 500 eV) lacks more and more obtainable energy resolution due to the fact that the initial states are Auger-broadened. Auger broadening also smears out structures in transitions in the outer s-shells²⁴ of the alkali halides (except Li^+1s). Therefore these states are omitted in Fig. 1.

Investigations of inner shell transitions in the energy range 10 to 500 eV bring about large experimental problems, especially concerning the lack of radiation sources and suitable radiation detectors for this spectral range. Technical developments, especially the use of synchrotron radiation, have helped to overcome these problems. Therefore some remarks on the characteristics of synchrotron radiation and on the experimental problems connected with the use of this source should be made before a review of the results of inner shell transitions will be given.

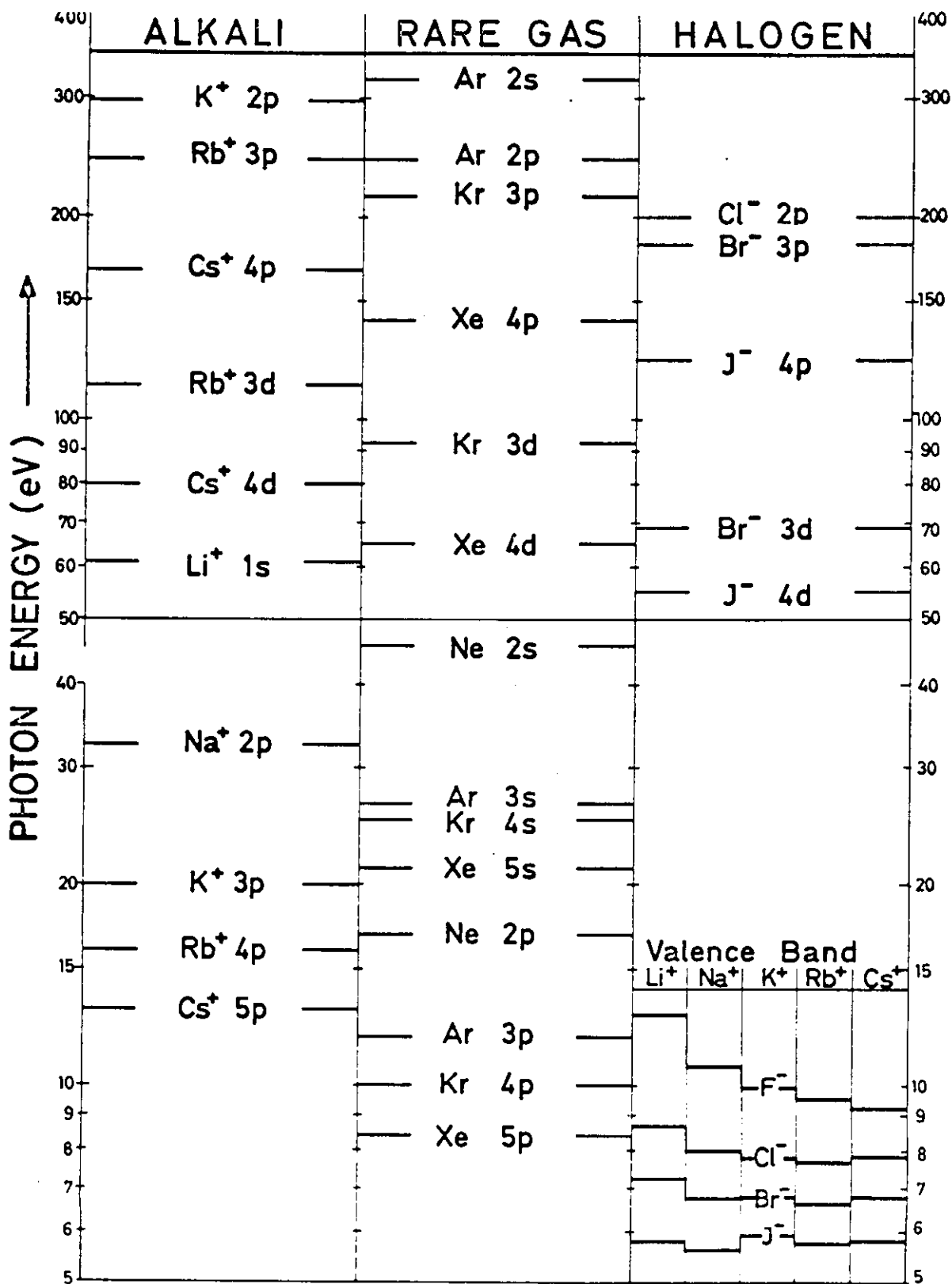


Fig. 1 Threshold energies for transitions from the different occupied shells in the alkali halides and rare gases. Each compound is indicated for the valence band transitions. For core levels the dependence of the chemical composition is small and therefore has been neglected.

III. SYNCHROTRON RADIATION

Synchrotron radiation is emitted by electrons centripetally deflected in bending magnets of high energy cyclic accelerators and storage rings. The radiation has a continuous spectral distribution extending from the radio wave region up to the ultraviolet or x-ray region dependent on the electron energy. Fig. 2 shows, as an example of spectral distribution the characteristics of the synchrotron radiation at the 7,5 GeV electron synchrotron DESY in Hamburg. The intensity is much higher than that of other sources especially of gas discharge continua and thus makes synchrotron radiation most suitable for absorption, reflection- and photoyield measurements in gases and solids. The high degree of polarization of the radiation is also very useful for solid state investigations. Table I summarizes the different accelerators where synchrotron radiation experiments have been performed or are in preparation. The basic parameters of the different accelerators (maximum energy E_{\max} , the magnetic radius R_m , λ_{\max} giving the spectral maximum, and the circulating current I) are included together with remarks on the experimental results published so far. The theoretical basis for synchrotron radiation may be found in textbooks.^{25,26} An extended development of the theory as based on the classical electrodynamics by Schwinger²⁷ and on the quantum mechanics by Sokolov et.al.²⁸ has been given. General descriptions of the characteristics of synchrotron radiation at different accelerators can be found in references²⁹⁻³¹.

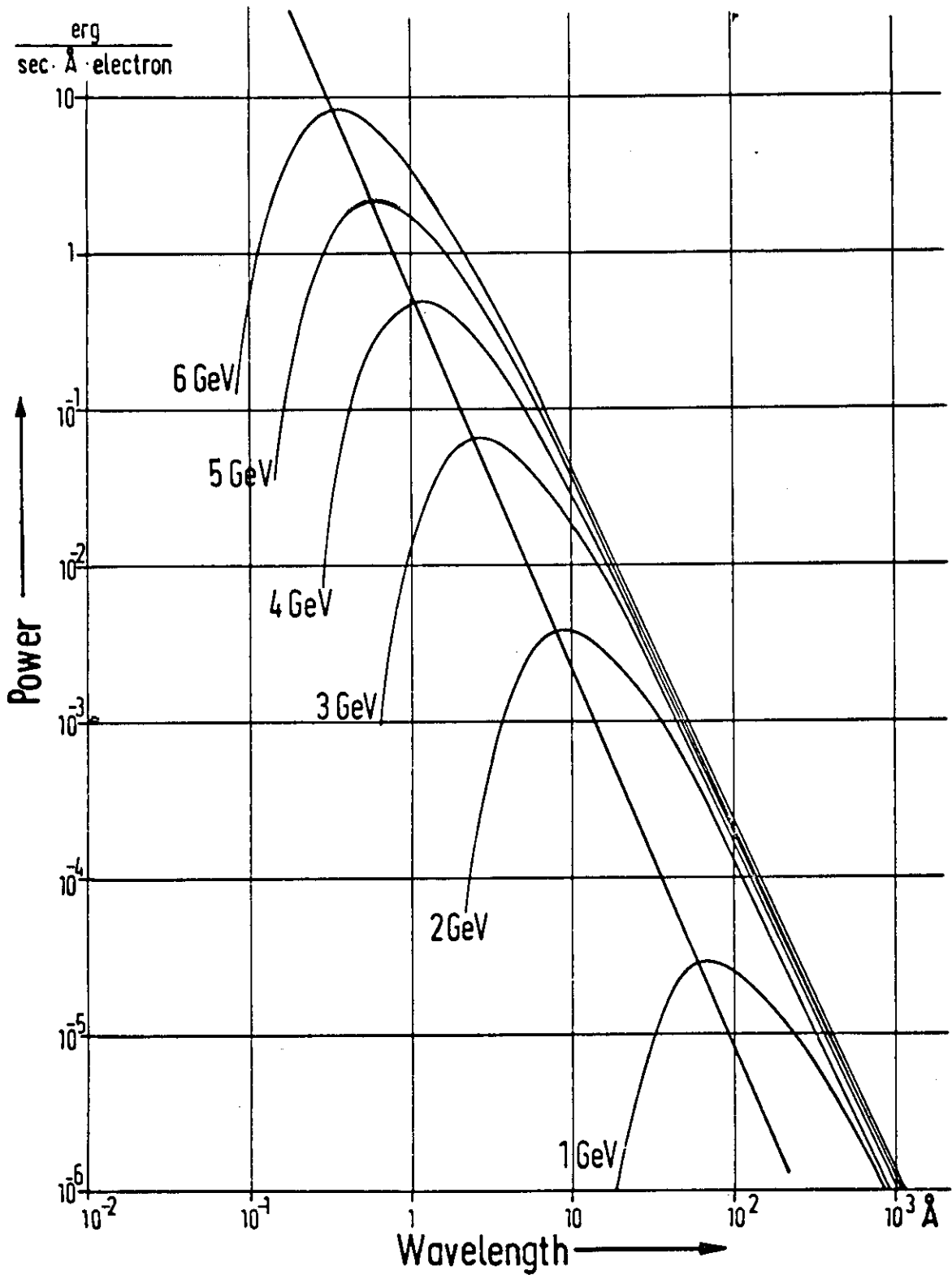


Fig. 2 The spectral distribution of the synchrotron radiation emitted by electrons of different energies at DESY.

As the synchrotron radiation has a very small angular dispersion around the instantaneous electron flight direction it is usually taken from a beam pipe mounted tangentially on the electron orbit in a bending magnet and led to the spectrometers several meters apart from the tangential point. In Hamburg and Tokyo, where the data, to be reviewed in the next chapter, have been taken, different spectrometers in normal and in grazing incidence have been used. At DESY photomultipliers have been used for radiation detection, whereas in Tokyo photographic films have been used. The latter does not allow exact intensity measurements, so that the evaluation of quantitative absorption coefficients is difficult. On the other hand they register the whole spectrum simultaneously and therefore are insensitive to current fluctuations in the accelerators which need intensity normalization procedures during scanning of the absorption spectrum with photomultipliers. These current fluctuations are a special problem in synchrotrons but will not play an important role in storage rings, such as the one in Stoughton, where alkali halide experiments are being performed by a group from the University of Illinois.³² At accelerators in the GeV (10^9 eV) range the spectrum of synchrotron extends to the x-rays (in the 100 keV-region), thus causing background radiation. This background radiation can be suppressed by inserting a mirror between the source and the spectrometers, which only reflects wavelengths longer than a limiting wavelength which depends on the entrance angle. Beside this straylight, caused by the high energy background radiation, the continuous spectral distribution gives rise to background caused by light

Machine	E_{\max}	R_{magn}	λ_{\max}	I	Experimental Results published so far
Glasgow Linac	100 MeV	5 cm ^f	118 Å		
National Bureau of Standards NBS	180 MeV	0,83 m	330 Å		Rare Gases, N ₂ , Al, Al ₂ O ₃ , Sn
Wisconsin Storage Ring	240 MeV	0,54	92 Å	~1 A	
Glasgow Synchr.	330 MeV	1,25 m	82 Å		Ar, Kr, Xe
Frascati Synchr.	1,1 GeV	3,6 m	6,3 Å	9 mA	Heavy Metals
Tokyo Synchr.	1,3 GeV	4,0 m	4,3 Å	5 mA	Ar, N ₂ , Metals, Alkali-Chlorides AgCl, TlCl
Bonn Synchr.	2,3 GeV	7,65 m	1,5 Å	30 mA	
NINA Daresbury	4 GeV	20,8 m	0,76 Å		
CEA Cambridge/Mass.	6 GeV	26,0 m	0,3 Å		
DESY Hamburg	7,5 GeV	31,7 m	0,17 Å	10 mA	Metals, Solid Rare Gases, Alkali-Halogenides, Intensity Calibration

Table I: List of accelerators and storage rings where synchrotron radiation experiments are either being performed or are in preparation.

^fin a 70 kF superconducting magnet

which is reflected from the grating in higher orders. This higher order light can be suppressed by the choice of gratings having an appropriate reflection characteristic (entrance angle, blaze angle) and by the use of different filters.

IV. EXPERIMENTAL RESULTS FROM INNER SHELL TRANSITION MEASUREMENTS

IV.1 Initial state with p-symmetry.

As can be seen from Fig. 1 the core shells with the lowest threshold energy are the outer shells of the alkali ions. Cs^+5p has its threshold at 13 eV, Rb^+4p at 16 eV, K^+3p at 20 eV, and Na^+2p at 32 eV.

Transitions from the K^+3p -shell. Reflection measurements for investigation of transitions from the K^+3p -level have been performed by synchrotron radiation on KCl, KBr and KJ.³³ Blechschmidt et.al.³³ used the multi-angle reflection method to evaluate n and k , as well as ϵ_1 , ϵ_2 and $|\ln \frac{1}{\epsilon}|$ in the energy range 12 to 30 eV. At this range synchrotrons are not the only radiation sources available, but with synchrotron radiation it is easy to scan the photon energy spectrum continuously with high resolution over a wide range. In addition measurements in parallel- and perpendicular-polarized light allow for checking consistency and accuracy of the data obtained. Stephan et.al.³⁵⁻³⁶ using a multiline capillary

discharge radiation source have made reflection measurements for 15° angle of incidence and a subsequent Kramers-Kronig analysis for an evaluation of KF, KCl and KBr in the energy range 5 to 45 eV. The results of both groups for KCl and KBr differ slightly in quantitative values but agree completely in the shape of the spectra as compared one to another and with results obtained from electron energy loss experiments made by Creuzburg³⁷ and Keil.³⁸ In the KF-results³⁴ a repetition of the valence band structures can clearly be seen in the K^+3p -transitions. In KCl and KBr the Γ_1 - and X_3 -excitons can clearly be seen at the beginning of each transition. The similarity of the rest of the absorption structure is not as great as in KF. There could be reasons for these differences: a) The initial states of valence band- and K^+3p -transitions are on different ions and the final state wavefunctions in the conduction band of KCl and KBr might be more inequally distributed on both ion types as in KF. b) The spin-orbit splitting of K^+3p is small (~ 0.27 eV) and the double peaks in absorption have not been resolved by Stephan et.al.³⁴⁻³⁶, but Keil in KBr³⁸ and Blechschmidt et.al. in KJ³³ see some indication of it in the Γ_1 -exciton. The valence band on the other side of KCl is split by 0.1 eV and of KBr by 0.5 eV, thus giving, in the case of KBr, double peaks in the valence band absorption, which would have to be unfolded before a comparison with the K^+3p -transition could be made, a problem which is difficult because of interaction between the transitions from the two valence band parts.

Transitions from the Rb^+4p and Cs^+5p -shell. The Rb^+4p and Cs^+5p -transitions have mainly been studied by Saito et.al.³⁹ The authors used a capillary discharge radiation source. Sharp peaks in the absorption spectra can be seen near the onset of the p-transitions (13 eV for Cs^+ , 16 eV for Rb^+) which can be correlated to Γ_1 - and X_3 -excitons.⁷

Transitions from the Na^+2p -shell. The onset of transitions from the Na^+2p -shell occurs in the sodium halides at about 32 eV. The absorption spectra of all sodium-halides have been studied at DESY with synchrotron radiation,⁴⁰ and bei Sagawa⁴¹ who used the quasi-continuum of a uranium rod spark radiation source, initially developed by Damany et.al.⁴² The NaCl should be discussed as representative for all sodium halides. Fig. 3 shows the DESY results as compared with results of measurements of Cl^-2p -transitions performed at the Tokyo synchrotron⁴³ and with data of valence band transitions obtained by Roessler and Walker.⁴⁴ At the onset of transitions in all three curves sharp structures can be seen superimposed onto a residual continuum, which is due to transitions from the valence band into high lying states of the conduction band. The peaks A and B in the Na^+2p -curve can be ascribed to both the Γ_1 -excitons. Their energy distance is close to the spin-orbit splitting value in the free ion of 0.2 eV. It is however remarkable that the height of A : B is not 2 : 1 as would be expected from the statistic contribution of the $2p_{3/2}$ and $2p_{1/2}$ shell, but 0,6 : 1 in NaF, 0,3 : 1 in NaCl, 0,47 : 1 in NaBr and 0,19 : 1 in NaJ. This inversion of the

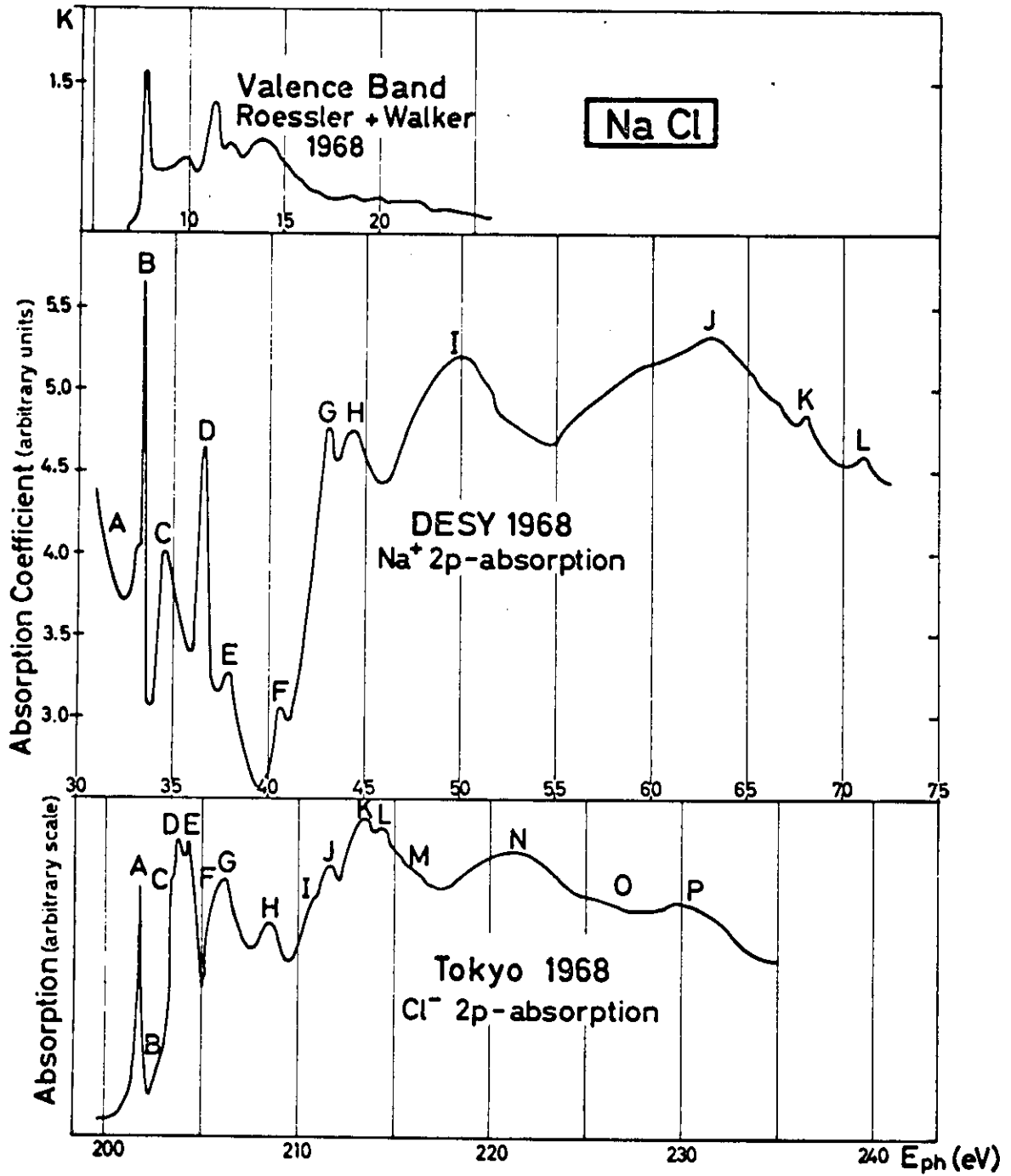


Fig. 3 Comparison of the absorption structure of NaCl for transitions from the valence band, Na⁺ 2p-level and Cl⁻ 2p-level.

oscillator strengths is explained by Onodera and Toyozawa⁴⁵ as caused by exchange interaction between the electron and the positive core hole. In Fig. 3 the energy adjustment of all three curves is made in such a way that the first exciton peaks coincide since no interband transition edges can be identified. The first peaks in all absorption curves are assumed to represent the Γ_1 -exciton, as Γ_1 is the lowest point of the conduction band.^{6,9,10} Fig. 4 shows the conduction band structure as obtained by A.B. Kunz⁶, extended by inclusion of the approximate position of the Na^+2p -level and the Cl^-2p -level. The next peak C (in Fig. 3) with the corresponding peak at 10 eV in the valence band absorption curve is believed to represent the X_3 -exciton. Its energy in the valence band as related to the Γ_1 -exciton is slightly higher than in the Na^+2p -transition. This can be explained from the fact that in the valence band the initial state X_7' is at a lower energy than at Γ_8' , the initial state of the Γ_1 -exciton, whereas the Na^+2p band is completely flat. The next peak D coincides with the 11.0 eV peak in the valence band absorption spectrum. This may lead to the assumption, that it may be a exciton coupled to a singularity at the Γ -point, i.e. Γ_{25}' although according to the results of A.B. Kunz⁶ it would require a somewhat higher energy. It should be pointed out, that the three band calculations for NaCl ^{6,9-10} differ not only in the position of energy, but also in the order of singularities at the different points in the Brillouin zone. These differences have been pointed out and the reason for them have been discussed by A.B. Kunz et.al.⁴⁶

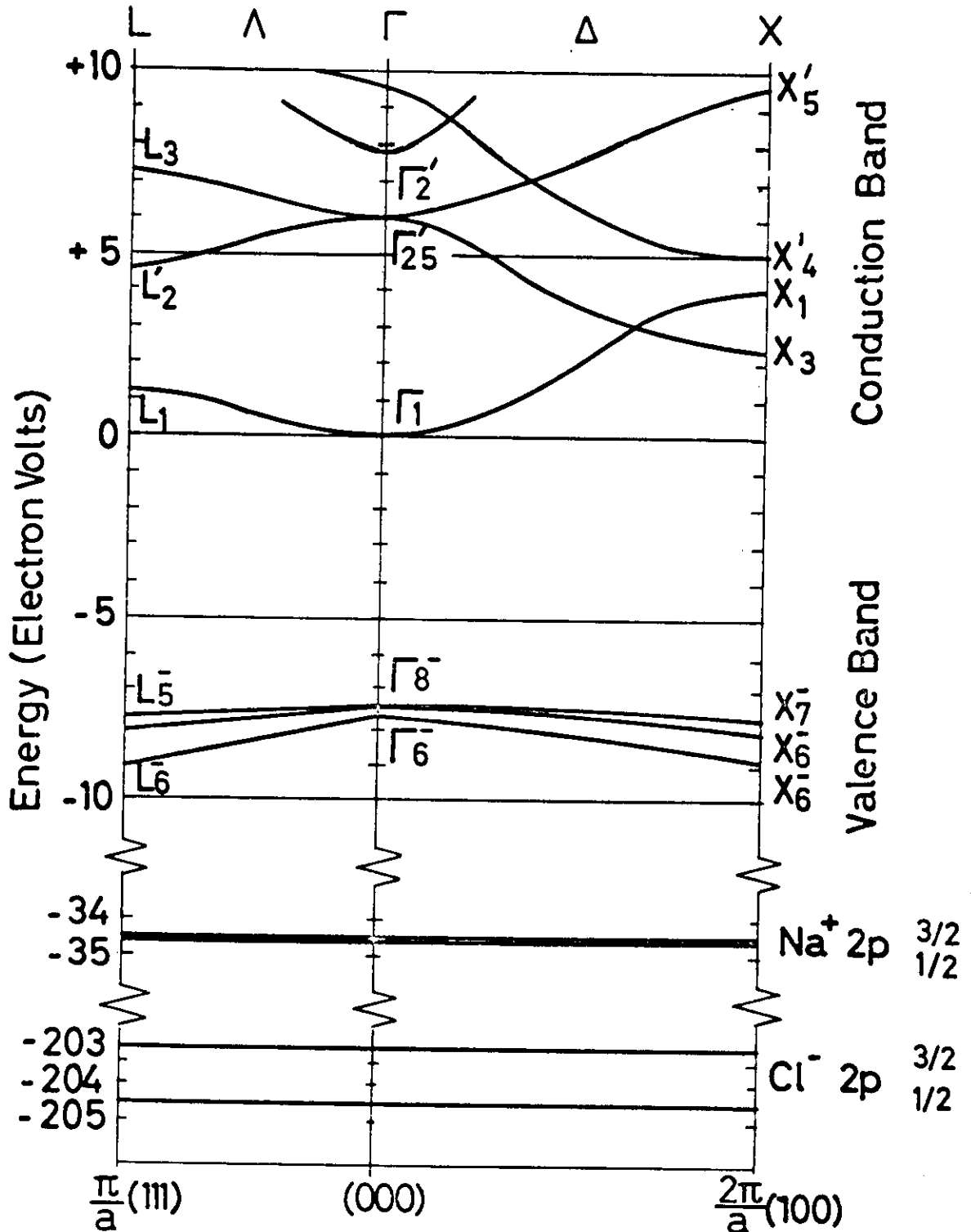


Fig. 4 Bandstructure of NaCl after A.B. Kunz⁶ with inclusion of the position of Na^+ 2p and Cl^- 2p. The zero-point of the energy scale has arbitrarily been positioned at the bottom of the conduction band.

About the role of two-quantum excitations. A step in the Na^+2p -absorption can be seen between F and G (Fig. 3), which can also be seen in similar forms in the other sodium halides and in the 2p-absorptions of all chlorides.⁴³ This steplike increase of absorption, which has no parallel in the valence band absorption structure, has been assumed by Iguchi et.al.⁴³ to be caused by double quantum excitation. In fact the step has an energy distance from the threshold which is equal to the band gap energy. It would therefore be energetically possible to have simultaneously excited one exciton or interband transition from the core- and one from the valence band level. Theoretical predictions of the oscillator strength of two quantum excitations^{47,48} are contradictory to each other.

Energy distribution measurements of photoelectrons of NaCl in the vicinity of the Na^+2p -threshold have been performed at DESY⁴⁹ to get additional information from experimental results. The results are shown in Fig. 5. The increase of the continuum intensity underlying the discrete structure can be ascribed to the distribution of the primary spectrum in the spectrometer, against which no normalization is possible as is the case in the absorption curve reduction. The appearance of all peaks up to 42 eV even at retardation potential up to -11 V shows that they are of excitonic nature, because interband transitions should yield photoelectrons with kinetic energies only up to ~ 8 eV. For retardation potentials higher than -8 V the structure from $E_{\text{ph}} = 43$ eV to higher photon energies is cut away edge-like at an energy distance from the 2p-transitions onset at 34 eV, which is equal to the retarding potential. This indicates, that here one-electron transitions play

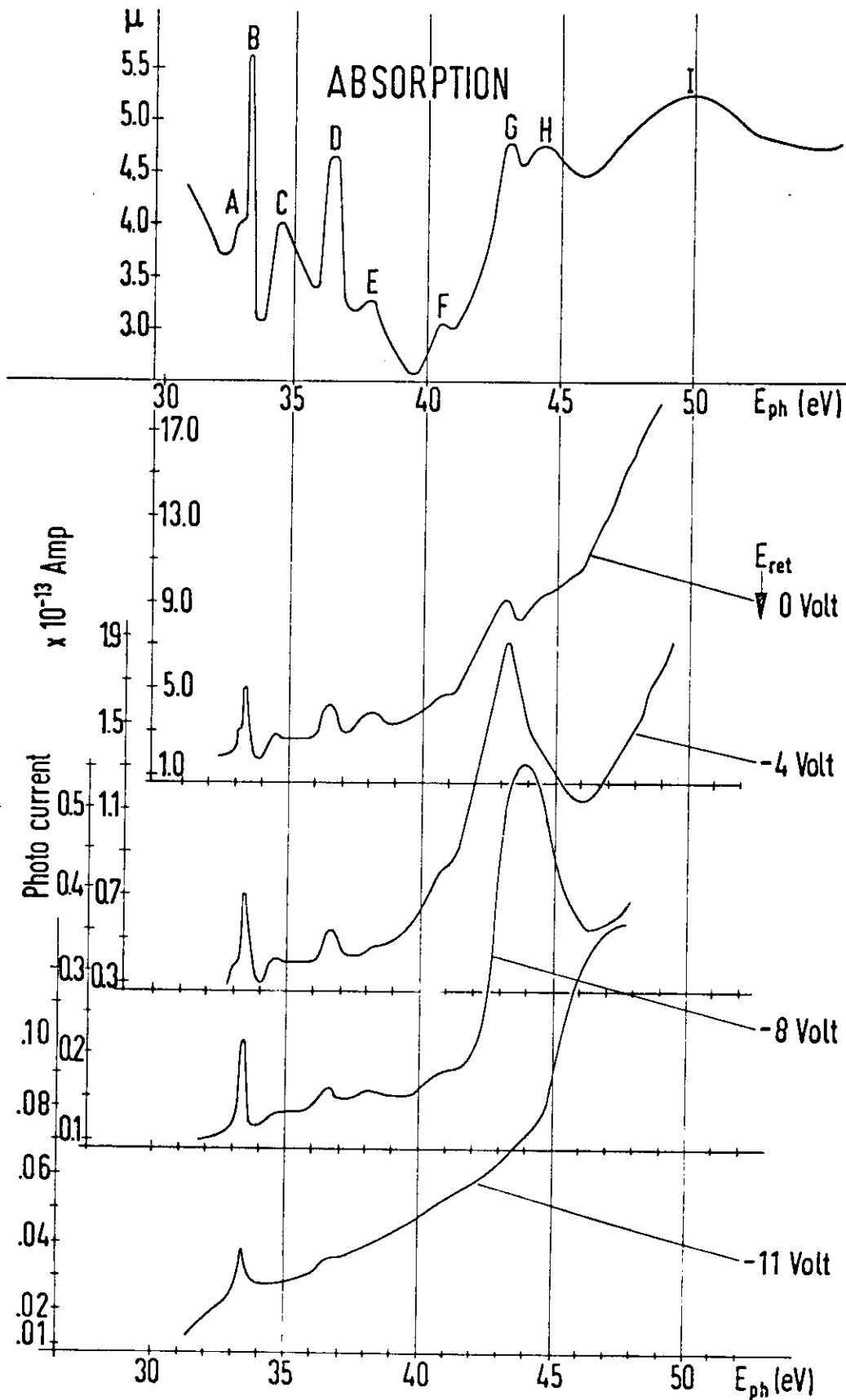


Fig. 5 Photoemission of NaCl in the vicinity of Na^+ 2p-transitions for different retarding potentials.

the main role since in the case of two-electron transitions both electrons would have low E_{kin} and therefore would already be suppressed by lower retarding potentials. Peak G at 43.0 eV is suppressed not so much by small retarding potentials as the peaks at higher photon energies. This shows that it is lying at an energy just below the onset of inelastic scattering.

Thus in our opinion, the double-exciton- or double-electron-excitation can be excluded as an explanation for the absorption step near 43 eV.

IV.2 Initial state with s-symmetry

Transitions from the $\text{Li}^+ 1s$ -shell. The investigation of initial states which have no p-symmetry gives us the possibility to study complementary states in the conduction band. The onset of transitions from the $\text{Li}^+ K$ -shell is at about 60 eV. The absorption behaviour of these transitions has been studied at DESY for all lithium halides.⁵⁰ The theoretical band calculations of the lithium halides⁵⁻⁸ indicate that the L_1 -point is very close to the Γ_1 -point. In LiCl and LiBr it is slightly above, in LiF and LiJ it is even below Γ_1 , thus making L_1 the lowest point in the conduction band. This has an important result because only where L_1 is the lowest point is it an M_0 -point,⁵¹ to which normal excitons can be coupled. The even parity of L_1 is only valid if the origin of the Brillouin zone is in the halogen ion. For the origin in the alkali ion the parity is changed, a fact which is valid for all points at L .^{4, 52}

Comparison of the experimental data on Li^+1s -transition with valence band transition is mainly possible for LiF , where, in the fundamental absorption region, data are available up to 25 eV from Roessler and Walker,⁵³ whereas for the other Li -halides data are only available near the threshold.⁵⁴ The band structure of LiF has been calculated by Kunz, Miyakawa and Oyama,⁵ who also from the theoretical point of view, made a comparison of the experimental valence-band and Li^+1s -transition data (see Fig. 6) also including electron loss data.³⁷ The first peak in the valence band data is ascribed to the L_1 -exciton, L_1 being the lowest point of the conduction band. As the wavefunctions of L_1 are highly concentrated around the halogen ion, transitions from the $1s$ -level of Li^+ , although allowed by the optical selection rules, are very weak and show up in the $1s$ -transitions only as a small shoulder A. It should be noted that LiJ^8 , also having the L_1 lower than Γ_1 , shows a similar shoulder at the onset of a higher absorption peak.⁵⁰

Then the $1s$ -transitions show a prominent absorption peak B, which is ascribed⁵ to an exciton at the p-symmetric X_4^1 -point but it should be pointed out, that the energy difference A - B is much smaller in the experiment, than should be expected from theory. It should be noted, that, according to Moore⁵⁵, the excitation energy of the free Li^+ ($1s^2 \rightarrow 1s2p$) is around 61,3 eV and therefore very close to A and B. The other structures may be either excitons or interband transitions, but their assignment in view of the band structure is difficult. However, it is remarkable that, except for peak D the rest of the structure has a similar

shape, despite the fact that both transitions come from states of different symmetry, localized at different ion types. An important proof of the energy adjustment of the two curves in Fig. 6 would be a measurement of the LiF-emission, which would directly show the energy difference between the valence band and the Li^+ K-level. The transition should occur around 50 eV, but no results of emission measurements on LiF came to the authors knowledge.

Another check could be in the form of an independent measurement of the binding energy of the electrons in the different shells by the ESCA-method.^{55a} Although some examples are given in reference^{55a} of alkali halides electron binding energies, no values are found for the lithium halides.

Transitions from the Ne 2s- and Ar 3s-shell. Up to now we were only concerned with alkali halides. In solid rare gases measurements of inner shell transitions give the opportunity to directly compare the same transitions in the gaseous and solid state in contrast to the alkali halides, where no transitions from core states have been studied on vapours. In solid rare gases the weak van-der-Waals binding forces make one expect that there are major similarities in the absorption spectra, not only as far the position of absorption structures is concerned, but also with regard to the shape of the lines. For many years the synchrotron of the National Bureau of Standards has been used for extensive measurements of the autoionization levels of solid rare gases.⁵⁶ Different types of absorption profiles

have been identified and in collaboration with Fano and Cooper⁵⁷ ascribed to the interaction of the discrete states with the underlying continuum. In Ne 2s-transitions⁵⁸ asymmetric and in Ar 3s-transitions⁵⁹ "window" type absorption profiles have been found. Although some evidence of asymmetric line shape has also been seen in different solids⁵¹, it seemed especially interesting to see if and to what extent characteristic line shapes in gases could also be seen in the solidified rare gases. First results obtained at DESY⁶⁰ indicate, that the asymmetric absorption lines in Ne 2s can also clearly be seen in the solid, somewhat broadened and shifted by 3 eV to higher energies. In Ar 3s one "window" type line has also been seen.

IV.3 Initial state with d-symmetry

Transitions from the Kr 3d-shell. The band calculations for solid Kr²⁰ indicate that the lowest parts of the conduction band mainly consist of s- and d-symmetric states. The inversion of parity at L does not occur in the monoatomic solid. It is therefore interesting to investigate, to which points of the Brillouin zone excitons are coupled which may be found in the absorption spectrum. Elliot⁶¹ has shown that two types of exciton transitions exist. The first are the "allowed" exciton series, formed between initial and final states, where direct optical transitions are allowed by the selection rules (the normal case for the p-symmetric valence band and the lowest s- and d-symmetric parts of the conduction band). The second are the "forbidden" excitons, formed between states, where direct transitions are not allowed. Here all Rydberg series

members, except $n=1$ can be formed. The classical experimental example is the exciton series in Cu_2O .⁶²

Fig. 7 shows the absorption structure of solid and gaseous Kr in the region of the gas absorption lines.⁶³ The energy of the Kr gas lines has already been evaluated by Couling and Madden⁶⁴ and served as energy calibration for the DESY measurements. In solid Kr many peaks can be seen (also above the ionization limit in the gas) which can be correlated in pairs, the corresponding partners always having an energy difference of about 1.22 eV, the spin orbit splitting energy of the 3d-shell.⁶⁴ At the onset a weak peak A can be seen, superimposed onto a continuum absorption of valence electron transitions into high lying states of the conduction band. Then a very high peak B at 91.6 eV with its partner B' at 92.8 eV follows, which are very close to the first members of the gas transitions. Because of their shape and their energy position lines B, C and B', C' are supposed to be members of exciton series. As no transitions into the $n=1$ exciton of a exciton series coupled to the s-symmetric Γ_1 -point are allowed from the d-symmetric initial state it is assumed that B and B' are the $n=2$ members, C and C' the $n=3$ members of exciton families converging to the Γ_1 point at 92,2 eV and 93,4 eV.

In this way A could be the forbidden $n=1$ exciton. The binding energy B in the exciton series

$$E = E_0 - \frac{B}{n^2} \quad \text{with} \quad B = \frac{\mu}{\epsilon^2}$$

would be 2.5 eV and 2.3 eV which is somewhat higher than 1.73 eV

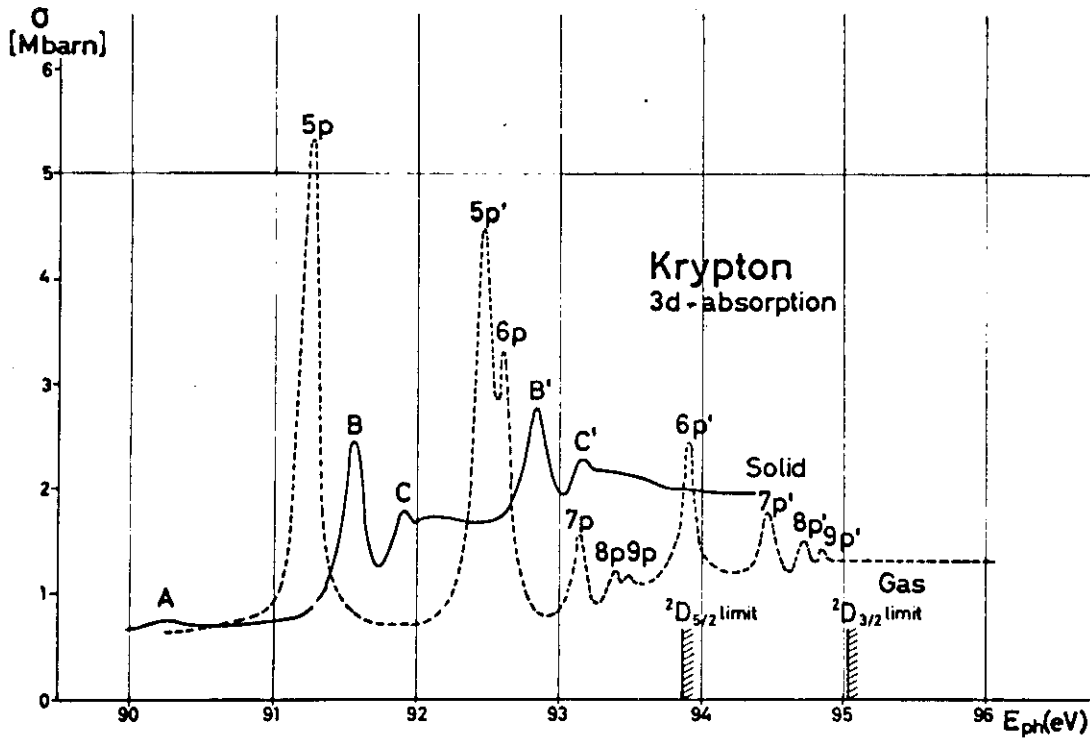


Fig. 7 Absorption of Kr in the vicinity of the 3d-threshold in solid and atomic state.

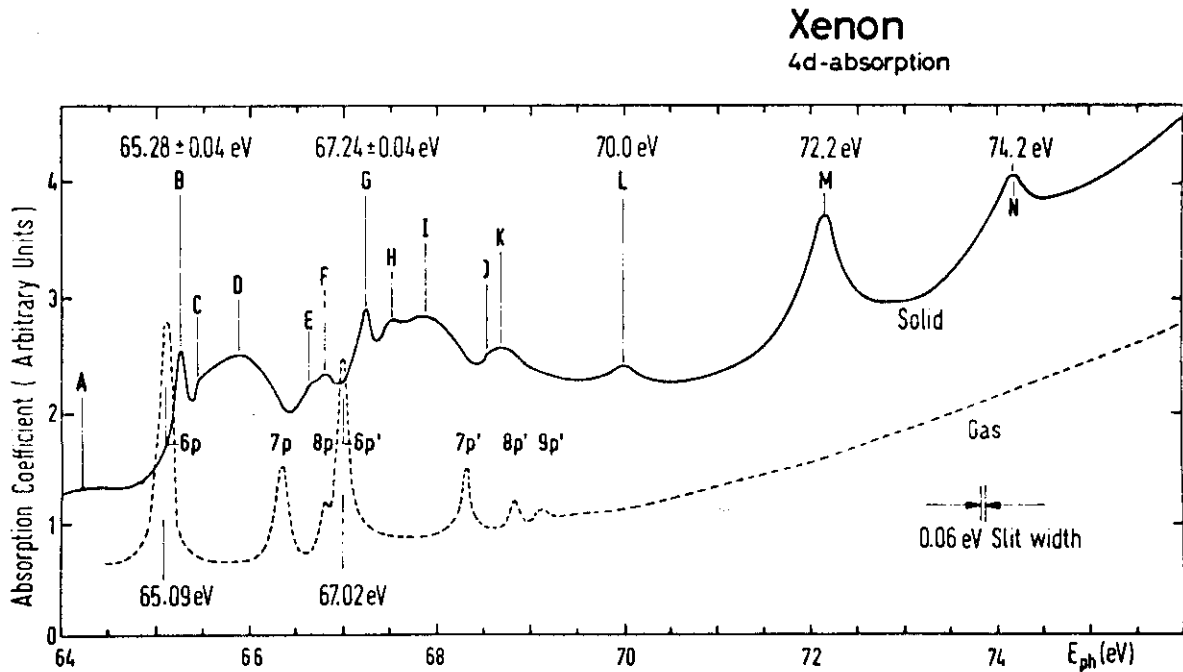


Fig. 8 Absorption of Xe in the vicinity of the 4d-threshold in solid and atomic state.

and 1.52 eV for the corresponding valence band excitons.⁶⁵ Assuming B and C to be the $n=1$ and $n=2$ members then B would have the small value of 0.5 eV. Another argument for the existence of a "forbidden" exciton series can be seen by comparing the oscillator strengths of B, B' and C, C' which are about 3:1. This is much closer to 2.6:1 theoretically predicted for $\frac{n=2}{n=3}$ of a "forbidden" series⁶¹, than 8:1 theoretically predicted for $\frac{n=1}{n=2}$ of an "allowed" series.

Transition from the Xe 4d-shell. A similar but admittedly less unambiguous identification of a forbidden exciton series can be made for Xe 4d⁶⁶ (Fig. 8), where A is also the forbidden $n=1$ exciton, B and G are the $n=2$ excitons and C and H the $n=2$ excitons. The latter are not so well separated as in Kr, since more structures are in the immediate neighbourhood. Thus we would be made to assume that in Xe higher conduction bands are closer to the bottom of the conduction band (the s-band with Γ_1 as the lowest point) than in Kr, which would be similar to the alkali halides, where, with increasing Z the higher conduction bands are attracted by the s-band. The band calculations of Kr²⁰ and Xe²¹, however, show very similar shapes as far as the distance of the s- and d-bands are concerned.

Beyond the first exciton series Xe shows a rich structure, where two peaks in the spin-orbit-splitting distance can always be correlated. These structures may be explained as excitons or (especially at higher energies) as interband transitions, but an unambiguous correlation is difficult. For further investigations

of the solid rare gases an extension of Baldini's valence band transition measurements⁶⁵ beyond 14 eV is highly desirable.

ACKNOWLEDGMENTS

The DESY experiments on which this paper is based have been performed together with Dr. C. Kunz of DESY and Mr. G. Keitel, Mr. P. Schreiber and Dr. B. Sonntag of the University of Hamburg. I would like to thank them for the stimulating and very pleasant collaboration, which made these experiments possible. For the communication of results of the potassium halide measurements prior to publication I would like to thank Mr. D. Blechschmidt, Mr. R. Klucker and Dr. M. Skibowski of the University of Munich. I am also grateful to the directors of the II. Institut für Experimentalphysik der Universität Hamburg and the Deutsches Elektronen-Synchrotron for their continuous interest and support of the synchrotron radiation group. Thanks is also due to the Deutsche Forschungsgemeinschaft for its financial support.

Literature:

1. R.S. Knox, Theory of Excitons (Academic Press, New York and London, 1963)
2. G. Baldini, Phys.Rev. 128, 1562 (1962)
3. F. Fischer and R. Hilsch, Nachr. Akad. Wiss. Göttingen, II. Math.-Physik Kl. 8, 241 (1959)
4. D.E. Ewing and F. Seitz, Phys.Rev. 50, 760 (1936)
5. A.B. Kunz, T. Miyakawa and S. Oyama (to be published)
6. A.B. Kunz, Phys.Rev. 175, 1147 (1968)
7. A.B. Kunz, Phys.Stat.Sol. 29, 115 (1968)
8. A.B. Kunz, (to be published)
9. T.D. Clark and K.L. Kliewer, Phys.Letters 27A, 167 (1968)
10. C.Y. Fong and M.L. Cohen, Phys.Rev.Letters 21, 22 (1968)
11. L.P. Howland, Phys.Rev. 109, 1927 (1958)
12. S. Oyama and T. Miyakawa, J.Phys.Soc.Japan 21, 868 (1966)
13. P.D. De Cicco, Phys.Rev. 153, 931 (1967)
14. Y. Onodera, M. Okazaki and T. Inui, J.Phys.Soc.Japan 21, 2229 (1966)
15. Y. Onodera, J.Phys.Soc. Japan 25, 469 (1968)
16. U. Rössler (to be published)
17. R.S. Knox, J.Phys.Chem.Sol. 9, 265 (1959)
18. R.S. Knox and F. Bassani, Phys.Rev. 124, 652 (1961)
19. L.F. Mattheis, Phys.Rev. 133, A 1399 (1964)
20. W.B. Fowler, Phys.Rev. 132, 1591 (1963)
21. M.H. Reilly, J.Phys.Chem.Sol. 28, 2067 (1967)
22. R.S. Knox and K. Teegarden in Physics of Color Centers, ed. W.B. Fowler (Academic Press New York and London, 1968)
23. J.A. Bearden and A.F. Burr, Rev.Mod.Phys. 39, 125 (1967)
24. D.H. Tombouljian in Handbuch der Physik XXX, ed. S. Flügge (Springer-Verlag, Berlin, Göttingen, Heidelberg, 1957) p. 294
25. J.D. Jackson, Classical Electrodynamics (John Wiley & Sons, Inc. New York and London, 1962)
26. R.P. Feynman, R.B. Leighton and M. Sands, The Feynman Lectures on Physics, Vol. I. chap. 34-3 (Addison-Wesley Publishing Comp., 1965)

27. J. Schwinger, Phys.Rev. 75, 1912 (1949)
28. A.A. Sokolov and J.M. Ternov, Synchrotron Radiation (Akademie-Verlag, Berlin, 1968)
29. K. Codling and R.P. Madden, J.Appl.Phys. 36, 380 (1965)
30. R. Haensel and C. Kunz, Z.Angew.Phys. 37, 3449 (1966)
31. R.P. Godwin in Springers Tracts in Modern Physics, Vol. 51; ed. G. Höhler (Springer-Verlag 1969) (to be published)
32. F.C. Brown, A. Fujita and Ch. Gähwiller (private communication)
33. D. Blechschmidt, R. Klucker and M. Skibowski (to be published)
34. G. Stephan and S. Robin, C.R. Acad.Sci. 267, 1286 (1968)
35. G. Stephan and S. Robin, Opt.Comm. 1, 40 (1969)
36. G. Stephan, E. Garignon and S. Robin, C.R.Acad.Sci. 268, 408 (1969)
37. M. Kreuzburg, Z.Phys. 196, 433 (1966)
38. P. Keil, Z.Phys. 214, 266 (1968)
39. H. Saito, S. Saito, R. Onaka and B. Ikee, J.Phys.Soc. Japan 24, 1095 (1968)
40. R. Haensel, C. Kunz, T. Sasaki and B. Sonntag, Phys.Rev. Letters 20, 1436 (1968)
41. T. Sagawa and S. Nakai, J.Phys.Soc. Japan 26, 1427 (1969)
42. H. Damany, J.-Y. Roncin and N. Damany - Astoin, Appl.Opt. 5, 297 (1966)
43. Y. Iguchi, et.al., Sol.State Comm. 6, 575 (1968)
44. D.M. Roessler and W.C. Walker, J.Opt.Soc.Am. 58, 279 (1968)
45. Y. Onodera and Y. Toyozawa, J.Phys.Soc. Japan 22, 833 (1967)
46. A.B. Kunz, W.B. Fowler and P.M. Schneider (to be published)
47. T. Miyakawa, J.Phys.Soc. Japan 17, 1898 (1962)
48. J.C. Hermanson, Phys.Rev. 177, 1234 (1969)
49. R. Haensel, G. Keitel, C. Kunz, G. Peters, P. Schreiber, and B. Sonntag (to be published)
50. R. Haensel, C. Kunz and B. Sonntag, Phys.Rev. Letters 20, 262 (1968)

51. J.C. Phillips, in Solid State Physics Vol. XVIII, ed. F. Seitz and D. Turnbull (Academic Press, New York and London, 1966) p. 56
52. P.M. Scop, Phys.Rev. 139, A 934 (1965)
53. D.M. Roessler and W.C. Walker, J.Phys.Chem.Sol. 28, 1507 (1967)
54. K. Teegarden and G. Baldini, Phys.Rev. 155, 890 (1967)
55. C. Moore, NBS Circular 467, I (1948)
- 55a K. Siegbahn et.al. ESCA Atomic, Molecular and Solid States Structure Studied by Means of Electron Spectroscopy (Almqvist & Wiksells Boktryckeri AB, Uppsala, 1967)
56. R.P. Madden and K. Codling, in Autoionization; Astrophysical, Theoretical, and Laboratory Experimental Aspects, edited by A. Temkin (Mono Book Corporation, Baltimore, Md., 1966) p. 129
57. U. Fano and J.W. Cooper, Rev.Mod.Phys. 40, 441 (1968)
58. K. Codling, R.P. Madden and D.L. Ederer, Phys.Rev. 155, 26 (1967)
59. R.P. Madden, D.L. Ederer and K. Codling, Phys.Rev. 177, 136 (1969)
60. R. Haensel, G. Keitel, C. Kunz and P. Schreiber (to be published)
61. R.J. Elliot, Phys.Rev. 108, 1384 (1957)
62. P.W. Baumeister, Phys.Rev. 121, 359 (1961)
63. R. Haensel, G. Keitel, C. Kunz and P. Schreiber (to be published)
64. K. Codling and R.P. Madden, Phys.Rev. Letters 12, 106 (1964)
65. G. Baldini, Phys.Rev. 128, 1562 (1962)
66. R. Haensel, G. Keitel, C. Kunz and P. Schreiber, Phys.Rev. Letters 22, 398 (1969)